



*Review*

## **Geodynamic factors in the formation of large gold-bearing provinces with Carlin-type deposits on continental margins in the North Pacific**

**Vadim Khomich<sup>1</sup>, Svyatoslav Shcheka<sup>2</sup> and Natalia Boriskina<sup>1,\*</sup>**

<sup>1</sup> Far East Geological Institute, Far Eastern Branch of Russian Academy of Sciences, 159 pr-t 100 let Vladivostoku, Vladivostok, Russia

<sup>2</sup> Macquarie University, Department of Earth and Environmental Sciences and ARC Centre of Excellence for Core to Crust Fluid Systems, North Ryde, NSW 2109, Australia

\* **Correspondence:** Email [boriskina2000@mail.ru](mailto:boriskina2000@mail.ru); Tel: +7-924-237-3038.

**Abstract:** Several similar indicators in Nevada (USA) and South Yakutia (Russia) gold-bearing provinces have been identified based on modern tectonic, geophysical and seismic tomography observations, followed by the analysis of the main geodynamic factors of the formation and distribution of large gold-bearing provinces in the North Pacific. One of the significant metallogenic peculiarities is a wide variety of formational and mineral deposits concentrated in the areas. Both provinces are situated at active margins surrounded by fold-thrust belts. In South Yakutia, a combination of sublatitudinal Baikal-Elkon-Ulkan and submeridional Seligdar-Verkhnetimpon gravity field gradient zones is recorded. In contrast, significant positive gravity anomalies of the Northern Nevada Rift and higher-order gradient zones are presented in Nevada. Large pluton and transform fault zones in both provinces support a conclusion about the fundamental role of geodynamic factors in developing ore-magmatic systems in the regions. Significant differences in the scale of the gold mineralization in the considered provinces are explained by the existence under the North American continent not only of the Mendocino transform fault zone but also of the Juan de Fuca paleo-spreading center. In contrast, the Inagli-Konder-Feklistov magmatic-metallogenic belt alone controls mineralization under the Asian continent.

**Keywords:** deep-seated geodynamics; Carlin-type deposits; transform fault zones; Nevada and South Yakutia metallogenic provinces

---

## 1. Introduction

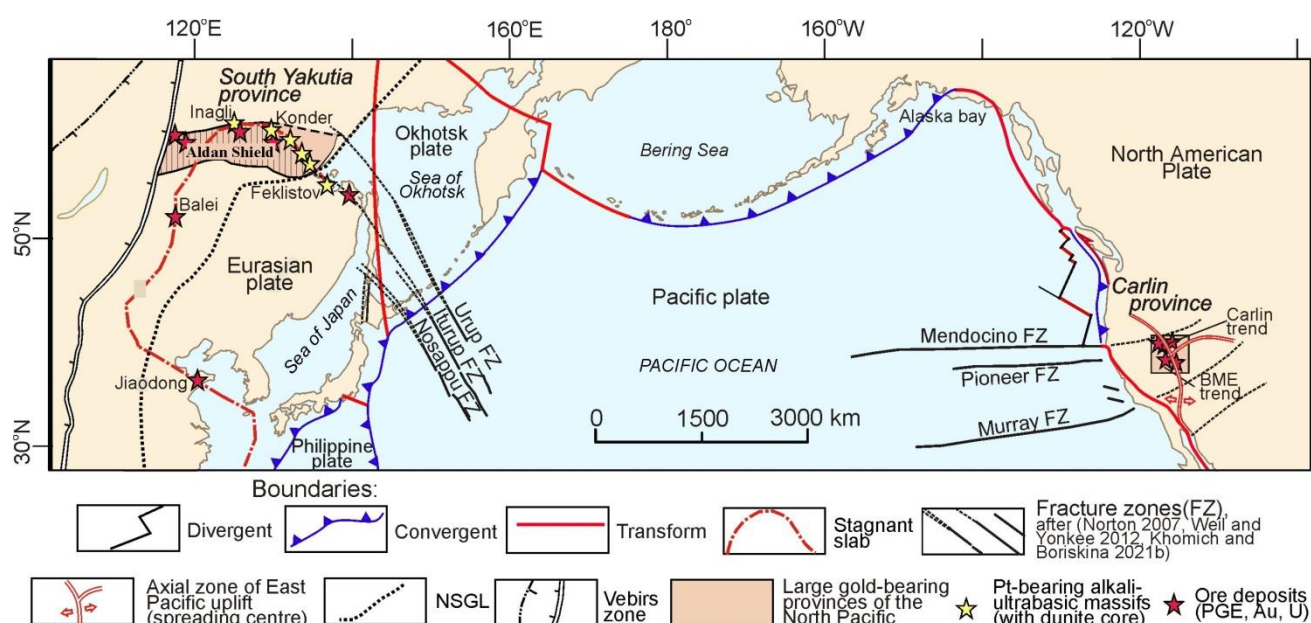
The Carlin metallogenic province (Nevada, USA) has become widely known as a gold ore region since the second half of the 20th century (Figure 1). More than 8000 t Au has already been mined [1]. The main sources of the noble metals in the province are large-volume hypogenic deposits, represented by finely disseminated supergene-transformed sulfide mineralization concentrated mainly within terrigenous-carbonate Proterozoic-Phanerozoic strata with elevated carbon content. The typomorphic mineralogical features of these deposits, generally called Carlin-type (or Nevada-type), include the presence of pyrite (especially arsenic), marcasite, arsenopyrite, stibnite, cinnabar, dispersed ionic gold, realgar, orpiment, native sulfur and arsenic, occasionally fahlores, bismuthine, barite and fluorite in the ores. Accordingly, geochemical aureoles of the mineralized areas are characterized by the presence of Au and compounds of Ag, Hg, Sb, Tl, Bi, etc., and high Au/Ag ratio. Ore deposits are usually distributed among jasperoids, areas of metasomatic silicification, calcification and argillization in the form of layered, sublayered or sometimes vein-like hydrothermokerst- and stockwork-like bodies.

A long period of intensive study of the Carlin ore-formational and geological-industrial deposits resulted in a relatively uniform interpretation of their presupergene origin as an important final stage of porphyry (magmatic-hydrothermal) gold-bearing systems that underwent extensive processing in oxidation zones [2]. However, along with a generally accepted interpretation of their genesis, numerous ideas about their geological diversity regarding age, association with certain magmatic systems, noticeable differences in physicochemical parameters of formation, distribution depth, etc., have been developed in recent decades [2,3]. The deposits of the so-called “Golden Triangle” Dian-Qian-Gui in southwestern China, second in the world after the Carlin province in terms of saturation with various types of Au mineralization, demonstrate the most pronounced deviations from the typomorphic characteristics of the Nevada-type deposits. However, the amount of gold mined here is still an order of magnitude lower than in Nevada [4].

There is another large gold-bearing province in Asia, where primary and placer Au deposits of various types, including gold-jasperoid deposits similar to Nevada, have been found. It is located in south-southeast Yakutia, Russia [5–10] (Figure 1). The most famous locality in the area is the Central Aldan ore-placer region. Several large-volume deposits of supergene-altered gold-bearing sulfide mineralization (Kuranakh Deposits) were discovered in the valley of the Bolshoy Kuranakh River (the right tributary of the Aldan River) in the late 1940s to early 1950s. Geological studies of gold deposits of various ore-formational and geological-industrial types within the Central Aldan and adjacent ore regions are in progress [7, 11–13].

For all of the abovementioned gold-bearing provinces of the North Pacific, most of the studies were focused on the influence of lithological, stratigraphic and structural-tectonic factors on the localization of mineralization, the determination of physicochemical and isotopic-geochemical indicators to explain the conditions of the formation of different types of Au deposits and the general direction of ore-forming processes. However, the importance of geodynamic processes responsible for the formation of distinct regional objects in the structure of the provinces, where deposits of the Carlin, Kuranakh and other geological and industrial types were identified [14], has been largely underestimated. In more detail, these data represent signatures of (a) paleo-riftogenesis in the regions that contributed to the accumulation of shallow-marine Proterozoic-Phanerozoic limestone deposits on the passive margins of cratons followed by (b) the development of orogen with the formation of

fold-thrust forms, (c) the large-scale appearance of proximal and distal magmatism on active margins, (d) the development of subduction and faulting and (e) multistage tectonic and magmatic activities. The role of supergene processes in the concentration of Au is also poorly understood.



**Figure 1.** Location of large gold-bearing provinces with Carlin-type deposits in the North Pacific. After [15–18] with some modifications and additions.

New information regarding the geodynamic settings of the gold-bearing provinces, regions and nodes, a determination of possible sources, and therefore the creation of modified geological-genetic, predictive models for the Nevada (Carlin, Kuranakh and others) type of mineralization, provided by modern geophysical and seismic tomography methods, was largely ignored until the last decade [14,19,20].

Here, we analyze the geological settings of the gold ore provinces, review the data from published tectonic, geophysical and seismic tomography studies of active margins of the North Pacific where trends, nodes, deposits and smaller ore bodies of Carlin-type and all the varieties of associated mineralization are concentrated and develop the main geodynamic factors of the formation of the aforementioned world-class gold-bearing provinces.

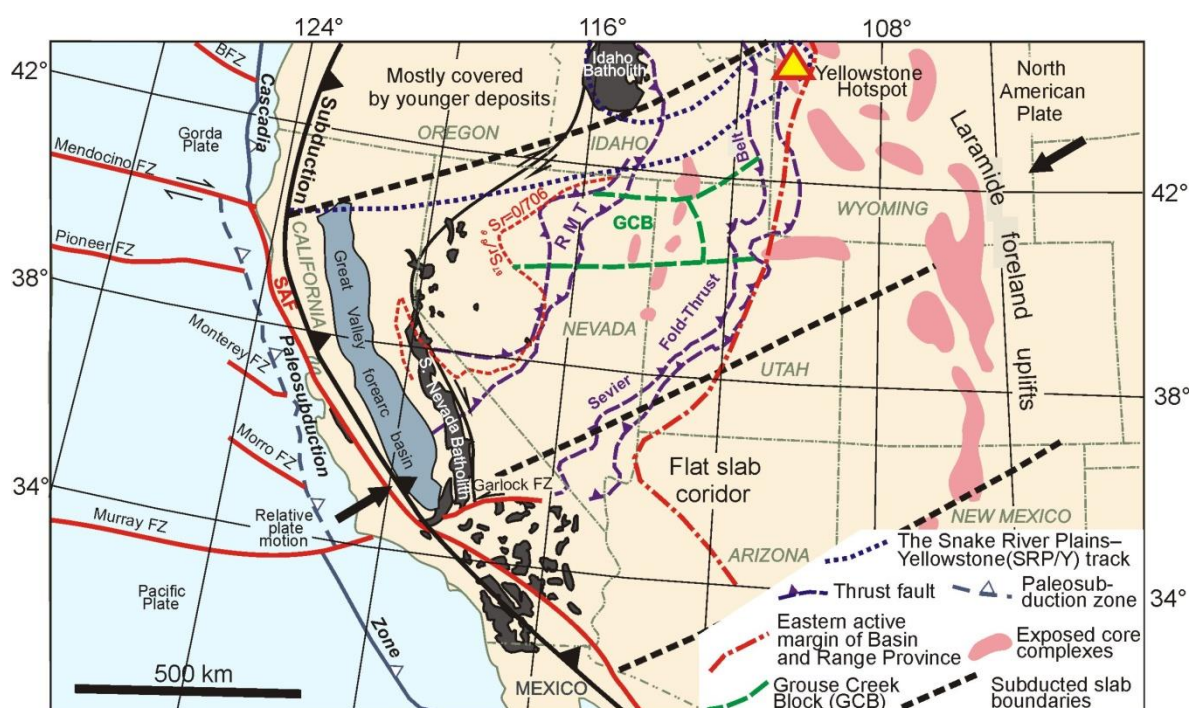
## 2. North Pacific gold-bearing provinces with Carlin-type deposits

The continental margins of the North Pacific are represented by complex accretionary orogens that have resulted from subduction, collision and sliding of young oceanic and ancient continental lithospheric plates [19,21].

### 2.1. Geological characteristics of the Carlin province (Nevada, USA)

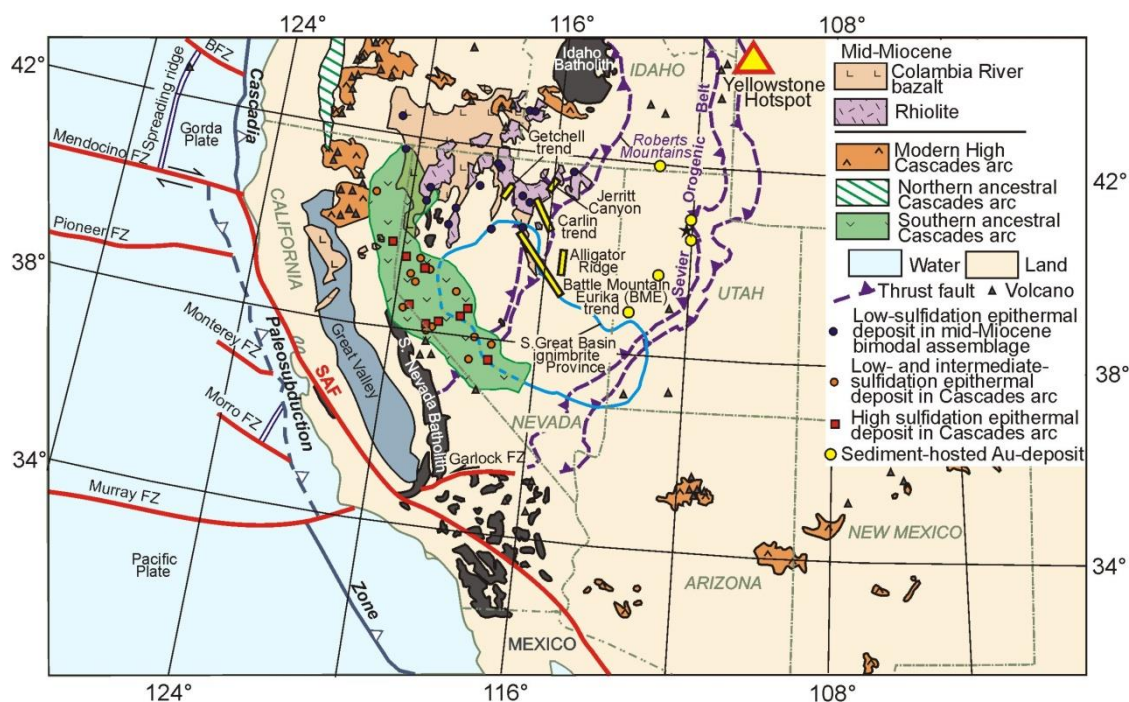
The southwestern (California-Nevada) part of the USA at the junction of the Pacific and the North American Platform with the Cordillera and Great Basin (Figure 2) is classified as a complex

accretionary orogen [19]. The geological history of this part of the USA includes continental rifting of Rodinia, accumulation of Proterozoic-Paleozoic and early Mesozoic terrigenous-carbonate siliceous-shale-calcareous strata at the passive margin, followed by the formation of the corresponding orogen in the late Mesozoic and Cenozoic ([22] see Figure 3), under the influence of compressional tectonics caused by the subduction of the young oceanic slab and the oncoming thrust faulting of the ancient continental plate. The impact of the Early Mesozoic (Middle Triassic) subduction processes predetermined the development of voluminous magmatism in the Earth's crust and the formation of the main magmatic arc. This is confirmed by the presence of I- and S-type plutonic rocks of Jurassic (160–140 Ma) and Cretaceous (120–80 Ma) age and associated W, Mo, Cu, Zn, Pb, Ag and Au porphyry deposits [18,22,23]. Later (~65 Ma), the area of plutonic magmatism migrated beyond the Great Basin toward the east. The extensional tectonic activity was accompanied by subaerial volcanism responsible for the formation of basalt-rhyolite bimodal assemblages in the middle Eocene (~45 Ma) followed by silicic caldera complexes and associated epithermal Au-Ag deposits with varying degrees of ore sulfidity in the Oligocene and Miocene [1,24]. The main elements of the Cordillera system are an accretionary wedge of sediments of the Franciscan series, a forearc basin, a magmatic arc including Idaho and Sierra Nevada batholiths, effusive pyroclastic deposits, ignimbrite fields and volcanic rocks of contrasting basalt-rhyolite formation [25], (Figure 2). Complex-dislocated Paleozoic–Early Mesozoic strata of the edge (pericratonic trough) of the North American Plate with Jurassic (Nevadan, Luning-Fence-maker, Elko) and Late Cretaceous (Seiver) orogenic belts [24,25] with dispersed Mesozoic-Cenozoic intrusive, subvolcanic and effusive formations are distributed east of the arc.



**Figure 2.** Schematic map of the Pacific coast of the United States combined with a tectonic map of the main components of the Late Cretaceous–Paleocene Cordillera orogenic system. After [25] with some modifications and additions after [17,19,26].

In north-central Nevada, two areas limited by thrusts and large allochthons are distinguished: early Mississippian (Robert Mountains) and Permian-Triassic (Golconda). Corresponding thrusts divide cross-sections of orogenic belts into autochthonous (carbonate-terrigenous) and allochthonous (siliceous-terrigenous interbedding with basic volcanic rocks), represented by Cambrian–Early Carboniferous (Preble, Hanson Creeks, Robert Mountains, Popovich, Rodeo Creek) and Ordovician -Triassic (Vinini, Grass Valley, Gray Blue, etc.) formations, respectively. It is believed that the autochthonous and allochthonous sequences were originally interconnected at the Antler Rise, which was a paleo-continental sedimentation zone in the transition from a geoclinal to a continental basin from the Cambrian to the Late Devonian [22]. The main Carlin-type deposit trends (Figure 3) and relatively large stocks of late Mesozoic granitoids (Gold Strike, Little Boulder Basin, etc.) are located in this zone. The Late Jurassic ( $160 \pm 3$ ;  $158 \pm 0.8$ ;  $157.7 \pm 0.4$ ;  $153 \pm 1$  Ma) diorite-granodiorite laccoliths are located in the southeastern part of the province (Robert Mountains ridge), in the Cortez ridge, between the Battle Mountain Eureka (BME) and Carlin trends, on the northern flank of the latter (Gold Strike intrusion) and within lamprophyre dikes surrounding laccoliths [27].



**Figure 3.** Geological and metallogenic map of the Western North American gold province with Carlin-type deposit trends (five yellow rectangles). After [17,24,26, 28–30] with some modifications and additions.

Small granite massifs located in the north-central part of the Carlin trend west of the BME trend and near the Getchell trend have Middle to Late Cretaceous ages ( $112 \pm 0.8$ ;  $96.3 \pm 0.6$ ;  $95.7 \pm 0.4$ ;  $95.2 \pm 0.6$ ;  $89.4 \pm 1.7$  Ma), respectively. Epizonal intrusions of granitoids [27] as well as stocks and dikes of rhyolites, dacites, andesites and sometimes basaltic andesites are widely present in the region and have Eocene ages varying from  $40.3\text{--}39.8 \pm 0.4$  Ma to  $35.2 \pm 0.2$  Ma. Ressel and Henry [27] assumed that an andesitic-basaltic paleovolcanic center (37.8 Ma) existed on the northern flank of the Carlin trend. They established synchronous migration of active magmatism centers of this age

southward and the possible presence of a wide (up to 12–23 km) and extended (approximately 50 km) paleo-magmatic chamber in the Earth's crust at a depth of 12–15 km [27].

Different parts of the province contain not only Late Jurassic, Cretaceous and Eocene diorite-granodiorite, granite hypabyssal massifs, stocks and mafic-felsic dikes but also long (up to 30 km) fields of volcanic rocks (Emigrant Pass, Robinson Mountain, etc.) with extrusive bodies, necks and effusive-pyroclastic accumulations up to 300–400 m thick and composed of multiple lava flows of andesites, dacites and dacitic and rhyolitic dikes.

Thus, the published data on magmatic formations in the Carlin province support the conclusions about the diffusive character of the late Mesozoic–Cenozoic magmatism developed in the area of the accretionary orogen in the rear and peripheral parts of the North American marginal-continental volcanic-plutonic belt.

Until recently, it was believed that the majority of Carlin-type deposits formed 42–36 Ma ago [3]. Many other types, including skarn and distal-disseminated Au deposits, have been assumed to be of the same age [14,22]. Popular in recent years [1], broad interpretation of the term “Carlin-type deposit” has led to the loss of clear lithological, stratigraphic, mineralogical and geochemical characteristics of this mineralization, on the one hand, and has allowed consideration of numerous data on its possible association not only with skarn but also with porphyry orogenic-type Au deposits, on the other hand. Recent publications [1] demonstrate the presence of not only jasperoids in the Carlin (USA), Dian-Qian-Gui “Golden Triangle” (PRC) and northern Vietnam provinces but also spatially adjacent Au-porphyry, Au-U, Au-Hg and Au-Cu-Mo-porphyry deposits [4,23,31] etc., characteristic of the South Yakutia (Russia) province [6–8,11,32,33], as shown below.

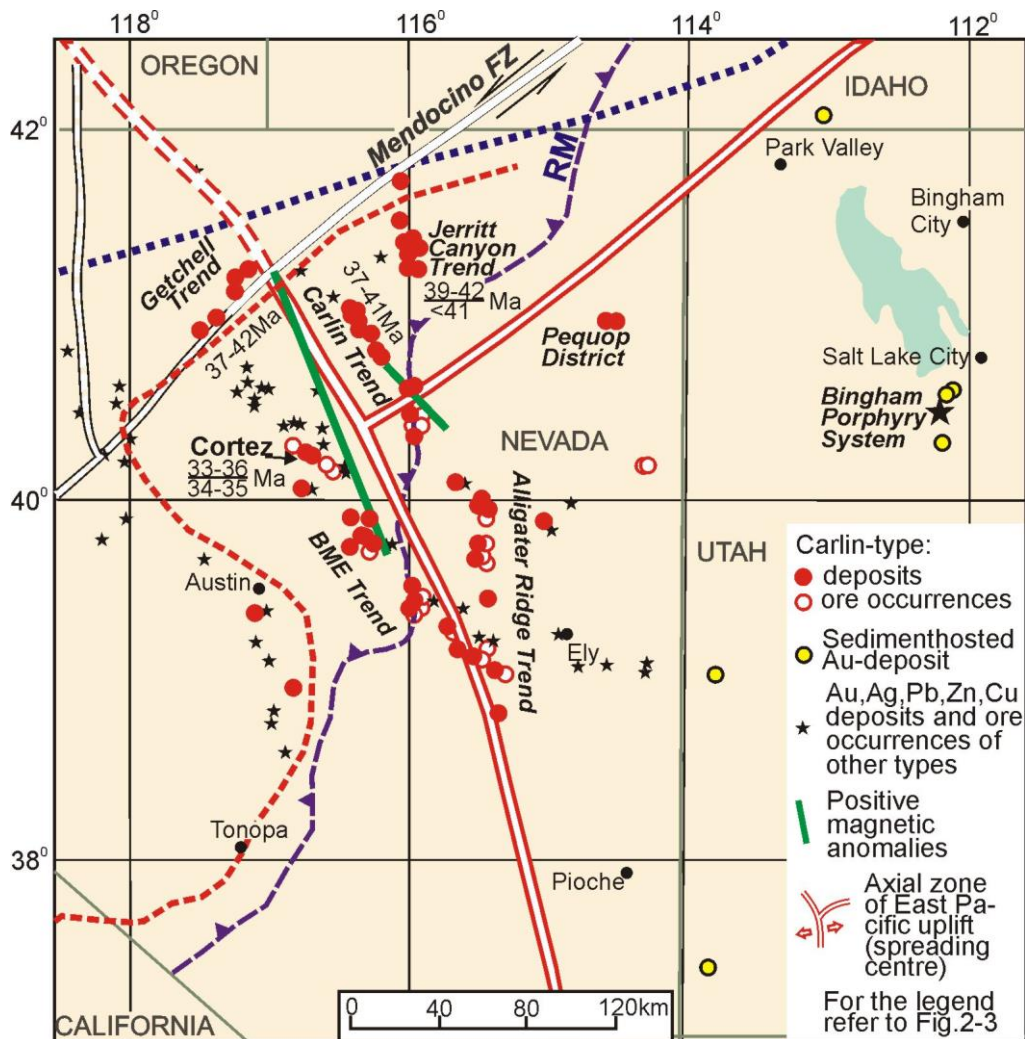
Decades of research on Carlin-type mineralization have resulted in detailed maps of individual deposits and their distribution trends (Figure 3). It is believed that the linear distribution of the Carlin-type Au-jasperoid deposits is largely predetermined by faults, initially concentrated in the Archean basement rocks but formed due to Neoproterozoic rifting [3,19]. Later, the faults were repeatedly reactivated during orogenesis and tectonic-magmatic activation. However, despite many empirical conclusions, predetermining a generalized genetic model for the evolution of mineralization in the province and geophysical and seismic tomography data provide additional argumentation to the model.

## *2.2. Geophysical characteristics of the Carlin gold-ore province*

The Carlin metallogenic province (Nevada, USA) is superimposed upon a large positive gravity anomaly called the “Northern Nevada Rift” ([34], see Figure 4). Its formation is explained by the rise of the mantle and the weakening of the Earth's crust, limited by local gradient zones [35] and corresponding deep faults similar to those common in the neighboring Cascadia subduction district [36]. Previously, long-lived thermal anomalies accompanied by numerous wellsprings formed by fluid and energy flows from the hot zone of the mantle [28] have been found in the province.

According to the Newmont Gold Corporation, the Nevada-type Au deposits are characterized by two intense linear magnetic field anomalies of the NNW orientation (Figure 4). Their projections fit into the regional magnetic anomaly generally concordant with the abovementioned gravity anomaly, local gradient zones [35] and the Carlin and Cortez (BME) trends. Processing and interpretation of gravimetry, magnetometry and thermometry data revealed Earth's crust structure and the thermal state of the California-Nevada-Wyoming part of North America. Jian Wang and Chun-Feng Li [26]

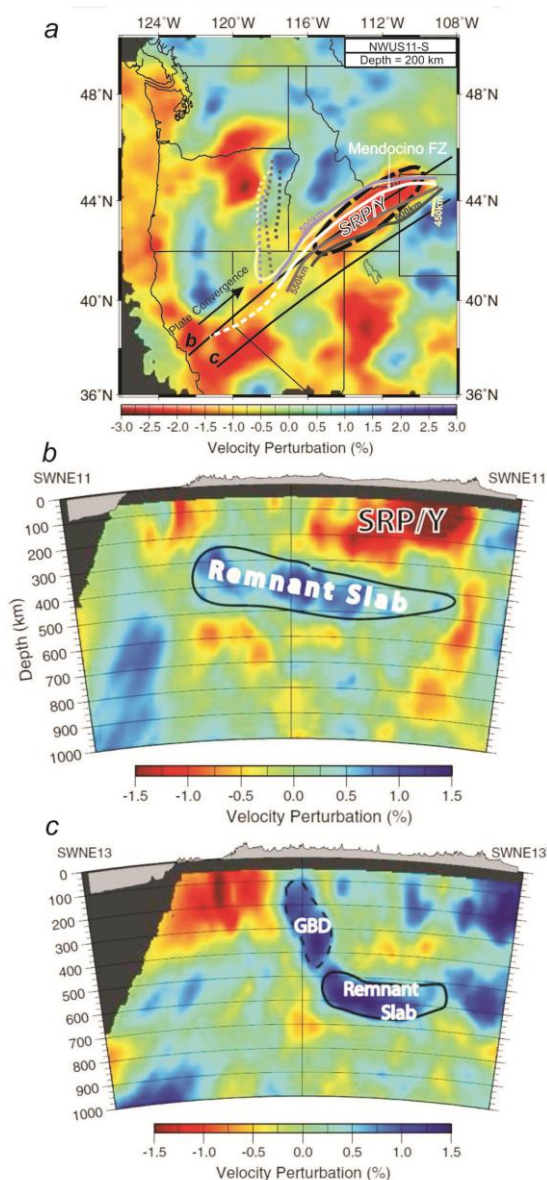
determined the degree to which Curie point (550 °C) positions differ in depth on opposite sides of the Yellowstone-Snake River Plain track–Yellowstone Hot Spot (SRP/Y). The geophysical differences were linked to the effects of Farallon plate subduction under the ancient continental North American plate and the possible interaction of fluid flows with the edges of the young slab. Activity along this track seems to be responsible for the origin of fluid channels, trench retreat and rising asthenospheric matter as toroidal (internal) and poloidal (ascending) upwelling embraces the Farallon slab. The Curie point depths, thermal lithospheric thickness and surface heat flows together establish the Paleogene North American Craton margin under the Roberts Mountains Thrust, marked by the  $^{87}\text{Sr}/^{86}\text{Sr}$  line (0.704–0.706 or 0.706–0.708) [14,19,26].



**Figure 4.** Location of the main trends and ore districts of the Carlin-type Au deposits relative to geophysical anomalies [6], geodynamic boundaries in Nevada (USA) and mineralization age [2]. After [17].

Seismic tomography research in recent decades [37–40] has shown that detailed high-definition S- and especially P-wave images of the Earth's crust and the mantle can reveal the presence of subducted oceanic plate fragments in the upper mantle and transition zone (Figure 5). Fault zone boundaries are distinguished by the contrasting conjugation of low- (slab gap) and high-velocity sections of S- and P-waves in the mantle [39]. This conjugation of sections with contrasting

velocities indicates the location of transform fault zones that divide the Farallon oceanic plate into fragments [37]. The neighboring positions of the Getchell, Cortez (BME), Carlin and Jerit Canyon trends in the northern part of the province correspond to the triple junction of the Mendocino transform fault and spreading axial trench of the Eastern Pacific rise.



**Figure 5.** Vertical P-wave velocity cross-sections parallel to plate convergence. After [39], with some modifications. Vertical cross-section profile lines (b and c) are keyed on the map view section shown in panel (a). Panel (b) is a vertical cross-section oriented along the axis of the SRP/Y hotspot track. It reveals a very gently NE-dipping (sub-horizontal) remnant of the Farallon slab in the mantle transition zone directly beneath the SRP/Y hotspot track, its leading edge just beneath Yellowstone. Panel (c) is a vertical cross-section along a transect south of the SRP/Y showing the southern continuation of the remnant slab as well as part of the Great Basin lithospheric drip (GBD). Multicolored lines with numbers 450, 500, 550 and 600 km show different NW borders of the remnant Farallon slab.

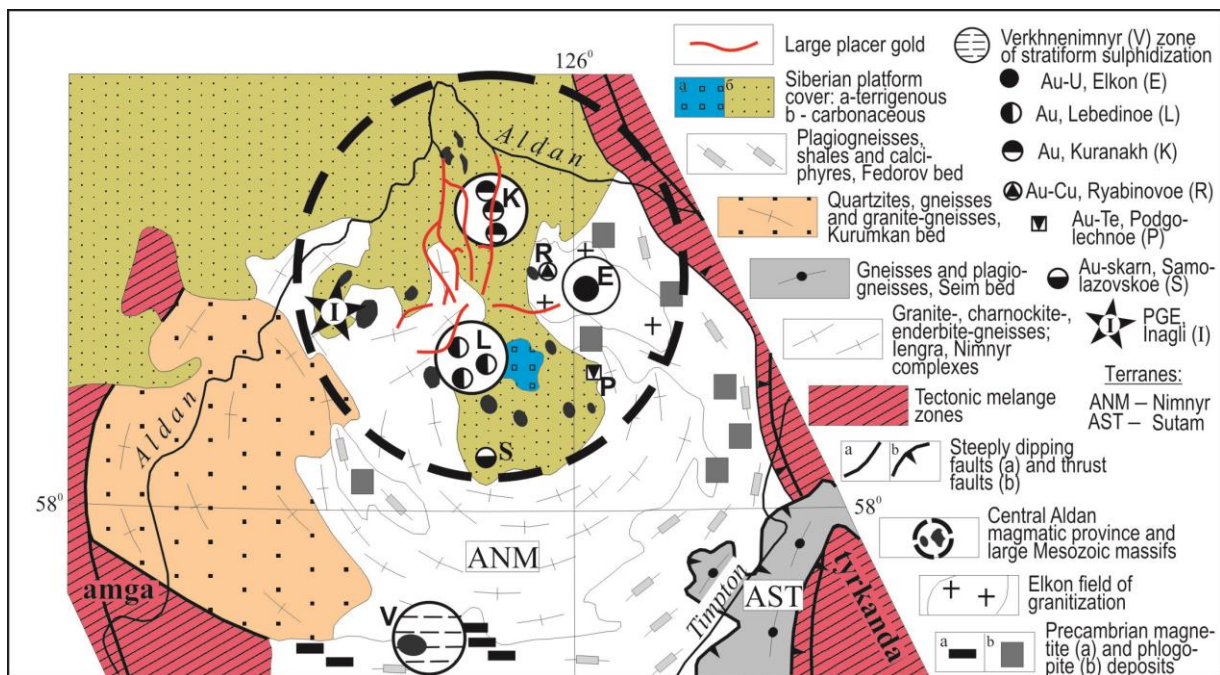


### 3. South Yakutia metallogenic province

Located on the southern flank of the Siberian Craton, South Yakutia Province is one of the most famous in Northeast Asia. Large and unique Precambrian and younger deposits of ferrous, nonferrous, noble, rare and rare-earth metals have been explored in the area [41]. A separate part of the province is the Aldan Shield, delimited from the Siberian Platform by the sublatitude Baikal-Elkon-Ulkan gradient zone of the global-scale gravity field. Three distinct superterrane, Olekma (West Aldan), Aldan-Timpton (Central Aldan) and Timpton-Uchur (East Aldan) (see Figure 1 in [42]), are identified within the Archean-Proterozoic basement of the shield.

#### 3.1. Geological characteristics of the South Yakutia

The Aldan-Timpton superterrane, also known as the Central Aldan ore region (CAR) (Figure 6), is the most saturated area with placer and primary Au deposits and has been mined for over 100 years.



**Figure 6.** Schematic map of Aldan-Timpton (Central Aldan) mineralized belt. Modified after [41,43].

Unlike the Carlin province (Nevada, USA), the CAR is characterized by the abundance of Au placers, the formation of which is predetermined by the geomorphological setting of the Cenozoic ensured the formation of unique reserves and parameters of complex deposits. They have varying compositions, the grain size of gold and different technological schemes of metal concentration and extraction [44].

Geological complexes of the Archean-Proterozoic crystalline basement and the Neoproterozoic-Cambrian platform cover, overlapped by Mesozoic terrigenous and effusive-pyroclastic accumulations, are combined in the CAR area. The stratified complexes of the cover and basement host many late Mesozoic multistage intrusive and subvolcanic massifs as well as ultramafic, alkaline earth, subalkaline, alkaline, ultraalkaline and felsic dikes, divided into comagmatic

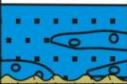









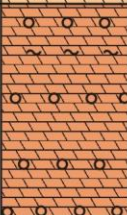

associations by age: Late Triassic–Early Jurassic, Middle Jurassic–Late Jurassic, Late Jurassic–Early Cretaceous and Early Cretaceous [41,45], named (not always with exact age boundaries) the Orochen, Aldan, Lebedinoe, Tobuk and Ket-Kap complexes, respectively [13,46–48]. There are several schemes of age and formation classification of the Aldan volcano-plutonic system [7]. The major associations are calc-alkaline trachyandesite-diorite-granodiorite, subalkaline monzonite-syenite, K-Na phonolite-alkaline syenite and two potassium associations: shonkinite-alkaline picrite and leucitite-alkaline syenite. Based on the determinations of the absolute age of the late Mesozoic magmatic formations, some of them are also identified in the Ketkap-Yun and Tomptokan regions of the eastern part of the Aldan Shield and with the Chara-Olekma terrane [47,49] in the west. Several time intervals of their formation were distinguished (Ma): 165–155, 145–140, 135–130 and 110–100 [48,50–52]. Dikes of alkaline rocks such as syenite-porphry, grorudite and tinguaitite crossing ore-bearing linear stockworks are the youngest.

The platform cover of the CAR (up to 600–650 m thick) is represented by subhorizontal terrigenous carbonate sediments of the lagoon and shallow-water facies. The epiplatform layer of the cover (up to 500 m thick in depressions) is composed of Jurassic gray and red conglomerates, gravelstones and sandstones of the Yukhtinskaya (J<sub>1-2</sub>) formation (Figure 7) predominantly preserved in linear grabens (Seligidar, Yakokut) originating from Precambrian narrow troughs (aulacogens?) where Neoproterozoic deposits are common.

The main geological feature of the CAR is the layered structure of the cross-section with numerous low-angle thrust faults, layered fault zones with tectonically dislocated contacts of intrusive massifs with stratified sediments, effusive-pyroclastic covers and subvolcanic sills and dikes [53]. A concentric arcuate distribution of derivatives of Mesozoic magmatism and ore mineralization is characteristic of the CAR [45].

In general, the metallogenic specialization of the CAR and the South Yakutia Late Mesozoic province is largely determined by Au, U, PGEs, Cu and Mo. In addition to unique Au placers, large gold ore clusters (Kuranakh, Lebedinoe, Elkon) and individual fields (Podgolechnoe, Ryabinovoe, Samolazovskoye) with deposits of different geological and genetic types, Au-jasperoid, Au-skarnoid, Au-sulfide (pyrite), Au-telluride, Au-porphry and Au-uranium, formed in a single metallogenic epoch are located in rocks of different structural levels.

Au-U mineralization of the Elkon cluster and Au-Te mineralization of the Podgolechnoe Deposit are concentrated in crystalline rocks of the basement (Figure 6). In the karst carbonate layers of the cover, there are subconcordant ribbon-like Au-sulfide (bottom of the section) and Au-jasperoid (top of the section) deposits of the Lebedinoe and Kuranakh nodes, respectively. Within the Late Mesozoic intrusive bodies, the gold porphyry mineralization of the Ryabinovoe Deposit and the Pt mineralization of the Inagli massif are concentrated. Mineralization of the Samolazovskoe Deposit is linked to sulfidized supergene and hydrothermally metamorphically altered tremolite-diopside-phlogopite skarnoids at the contact zone of aegirine-augite syenites with metamorphized dolomites [7].

SYSTEM	EPOCH	SUITE	STAGE	STRATA	INDEX	LITHOLOGY	MAX THICKNESS,m	ROCK DESCRIPTION	
Jurassic	Lower	Yukhtinskaya	Lower				40-70	Quartz-feldspar sandstones with lenses of conglomerates and gravelstones, interlayers of mudstones with flora	
Cambrian		Kutorginovaya	Upper		€ <sub>1</sub> kt <sub>2</sub>		80	Dark gray, banded, spotted, often <b>bituminous</b> limestones with rare interlayers of dolomites and detritus limestones with brachiopod fauna	
			Lower				20	Gray dolomites, detritus limestones with fauna	
		Ungelinskaya	Upper		€ <sub>1</sub> un <sub>2</sub>		35-40	Yellow-gray, gray dolomites with interlayers of brown clay dolomites, variegated marls of stromatolite dolomites and limestones	
			Lower		€ <sub>1</sub> un <sub>1</sub>		60-70	Variegated, thin platy marls with interlayers of brown, clayey green-gray dolomites, yellow-gray dolomites, stromatolite limestones; in the lower part - silicified dolomites	
		Tumuldurskaya	Upper	Upper		€ <sub>1</sub> tm <sub>2</sub>		40	Yellow-gray, gray dolomites with lenses, nodules of gray and dark gray flints, rarely marls
				Lower		€ <sub>1</sub> tm <sub>1</sub>		60	Gray, yellow-gray, spotted, often <b>bituminous</b> dolomite, stromatolite limestone interlayers and brown marl
			Lower		€ <sub>1</sub> tm <sub>1</sub>		35	Gray, yellow-gray bituminous dolomites with interlayers of dark gray <b>bituminous</b> and stromatolite limestones	
			Pestrozvetnaya			€ <sub>1</sub> pc		50-75	Variegated marls and marly dolomites, yellow and gray dolomites
	Vendian	Lower	Yudamskaya	Upper		€ <sub>1</sub> jd <sub>3</sub>		30-40	Sparkling grainy yellow dolomites, greenish gray and gray dolomites
				Middle		€ <sub>1</sub> jd <sub>2</sub>		160-200	Differently grainy gray dolomites, bituminous dolomites sometimes with gypsum, marly dolomites; in the lower part - silicified oolitic dolomites; in the upper part - dark gray oolitic dolomites
Lower					€ <sub>1</sub> jd <sub>1</sub>		20-40	Light gray dolomites, sandy dolomites; in the lower part-basal conglomerates and sandstones	

**Figure 7.** Stratigraphic scheme of Central Aldan ore district. After [6] with modifications and additions.

The gold-uranium mineralization of *the Elkton node*, located on the granitized basement ledge, is controlled by long (tens of km) ancient but reactivated faults, where the Early Proterozoic microdiorites interchanging with blastocataclasites and blastomylonites are surrounded by quartz-microcline and pyrite-carbonate-K-feldspar metasomatic bodies [32,43]. The absolute ages of metasomatites (150–130 Ma), brannerite (135–130 Ma) and postore dikes of alkaline rocks (125–103 Ma) have been measured (K-Ar, U-Pb method) [43]. Gold is concentrated in pyrites of metasomatites with some grains (30–50 μm, 700 ‰) found in the late calcite-adularia association [32].

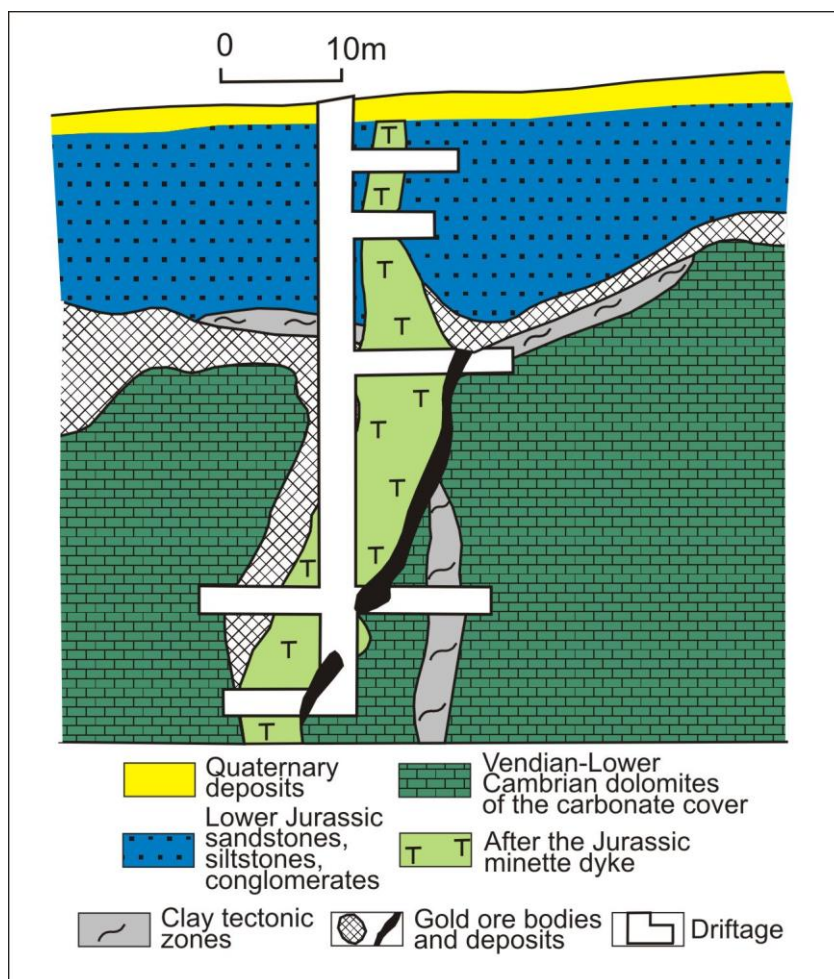
Gold-bearing deposits (isometric stockworks and linear subvertical mineralized zones) of *the Ryabinovoe ore field* were identified in the intrusive massif at the western margin of the Elkon rise. The massif consists of rocks of two different age phases: earlier leucocratic and later melanocratic rocks belonging to one bimodal antidromic high-K intrusive series [32,33]. The early, volumetrically dominant association is represented by aegirine-augite alkaline feldspar syenites and quartz syenites of the Aldan Complex (144–142 Ma) with syenite-porphry dikes ( $133 \pm 5$  Ma, [33]). The late association of the Tobuk Complex (130–141 Ma, [33]) consists of stock-like bodies and dikes of alkaline gabbroids, monzonitoids, melanocratic aegirine-augite syenites, phlogopite-pyroxene lamprophyres and eruptive breccias with lamproite cement.

*The Inagli ore-placer node* with the ring-zoned alkaline-ultrabasic Inagli massif with a 5.5 km diameter dunite core in the center is located in the western part of the CAR. Dunites of the central core are progressively replaced by olivinites (pyroxene-olivine rocks with variable amounts of micas), peridotites and pyroxenites, shonkinites and malignites, and pulaskites at the rim. The ages of zircons from dunites ( $134 \pm 1.8$  Ma) are similar to the Ar/Ar dating of amphibole ( $133 \pm 1$  Ma) sampled from amphibole-orthoclase pegmatite with chromium diopside [52] and are consistent with an earlier determination of the U-Pb age of zircons from the dunite core [54]. The platinum mineralization of the node, determined in idiomorphic grains of ferroplatinum from the placer by the Pt-He method ( $127 \pm 6$  Ma), has the same age [55].

Alkaline-ultrabasic ring massifs with a dunite core similar to Inagli (Konder, Chad, Sybakh) are also known in the East Aldan (Timpton-Uchur) superterrane [56]. The ages of the platinum-bearing dunite of the Konder massif (U-Pb method, baddeleyite-zircon system) are  $124.9 \pm 1.9$  and  $125.8 \pm 3.8$  Ma [57].

The gold deposits of *the Lebedinoe cluster*, represented by different geomorphological, geological and mineral-geochemical types, belong to one Late Mesozoic ore-magmatic system [7,13]. The ledges and elevated blocks of the basement among monzonite-syenite extrusive-subvolcanic bodies host deposits of the Au-sulfide type and lower levels of magma inlets of the massifs—Au-skarn and vein-types. The upper parts of the dolomite section contacting the massifs contain rich quartz-polysulfide deposits and veins. They are replaced by Au-pyrite-carbonate and Au-pyrite deposits and veins in subhorizontal and vertical paleokarst and hydrothermokarst cavities, respectively, at lower lithological-stratigraphic levels and with increasing distance from the massifs. Deposits of the Lebedinoe node, concentrated among the Vendian dolomites, are represented by two- or three-tiered deposits and steep bodies with subalkaline dikes in some areas (Figure 8). The total number of identified ore bodies exceeds 150. There are several mineral types of ores: two earlier (Au content  $< 20$  g/t)—pyrite-quartz-carbonate and pyrite-quartz and two later ( $> 20$  g/t)—hematite-pyrite-quartz and quartz-galena-chalcopyrite-pyrite-quartz (polysulfide). The concentration of pyrite in ore (from partially or entirely loose oxidized masses in the karst strata) varies from a few grains to 10–15% and up to 50–70% [13].

The highest Au content is observed in steep veins of variable morphology associated with fractured zones. Their length varies from the first ten to hundreds and thousands of meters. The usual thickness of the veins is 0.4–0.6 m, but they become conductors within magmatic formations (Figure 8).



**Figure 8.** Morphology of steeply dipping veins of the Lebedinoe Deposit. After [7].

Such quartz-polysulfide veins with Cu, Pb and Zn minerals associated with rich stratiform deposits of the upper levels are characterized by the presence of native Ag and Bi and, in general, an elevated content of Au and Ag: up to 50 and 400 g/t, respectively. Au concentrations reach 30 ppm in the areas of neighboring veins and dikes in syenite porphyry [13].

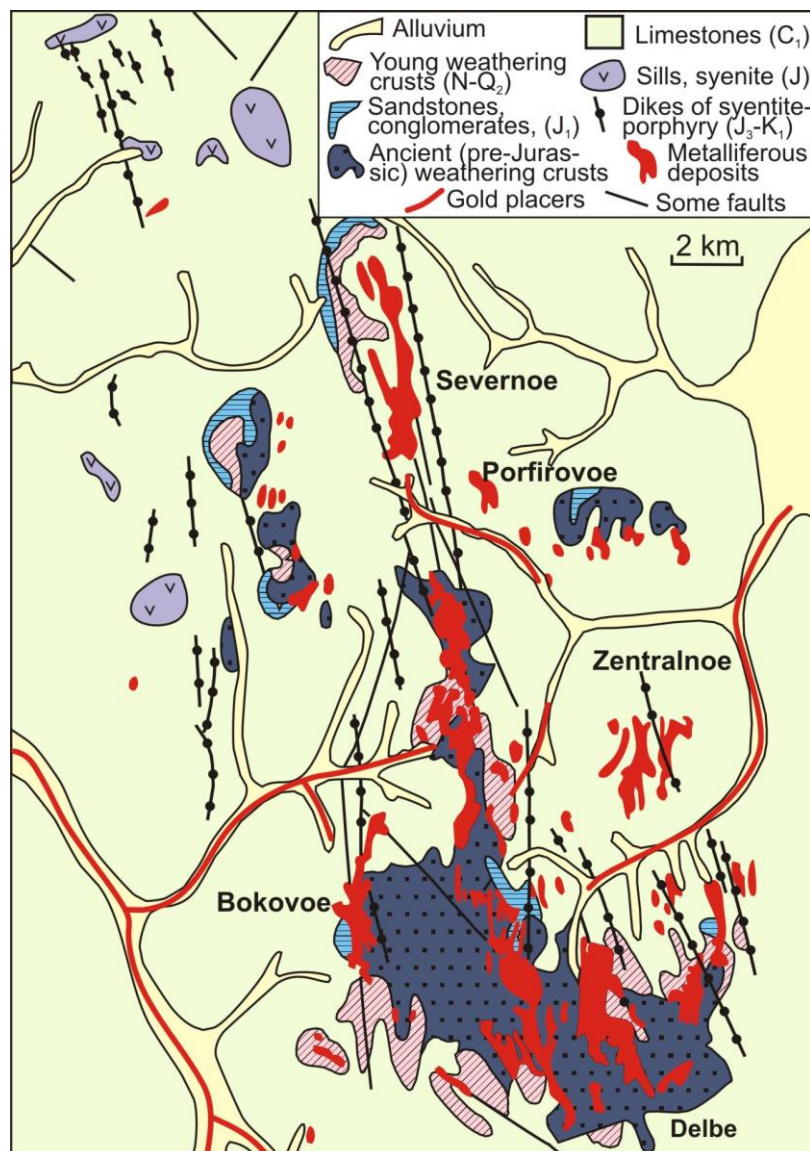
Paleo-karst cavities accompanying gold veins and deposits are common in the East Aldan superterrane. In the local East Aldan (Timpton-Uchur) metallogenic zone, several ore-placer regions and nodes are known: Tomptokan (Au), Dar'ya (Au-Ag), Dan' (Au), Omninsk-Odola (Au), Yun' (Au), Yurt (Au), Ulakhan (Au-Ag), Chad (Au-Pt), Konder (Pt) and others [6,56]. They are usually hosted by the Riphean-Cambrian terrigenous-carbonate strata of the Uchur-Maya depression and the eponymous massifs of the monzonite-diorite complex. The absolute age (K-Ar, U-Pb methods, from zircon and sphene) of magmatites with precious metal mineralization is 125.8–120.1 Ma [47].

The Tas-Yuryakh Au-sulfide-quartz deposit of the Kurun-Uryakh ore field in the Yudoma-Maya pericratonic trough near the eastern margin of the Siberian Platform is located in paleokarst cavities with gold mineralization. A system of ore-hosting flaky thrusts and reverse faults has developed here in the depression of the cover and basement of the platform [6,58].

**The Kuranakh node**, discovered in the late 1940s–early 1950s in northern CAR, is located between the Seligdar and Yakokut rivers [7]. The cluster is characterized by large deposits of ochred gold-bearing limonite-quartz ores, normally concentrated at the stratigraphic discordancy of

eluvial-deluvial breccia-like terrigenous ( $J_{1-2}$ ) deposits and carbonate ( $\epsilon_1$ ) strata of the sedimentary cover of the Siberian Platform (Figure 9). The deformed unconformity surface is overlapped by the Jurassic ( $J_{1-2}$ ) terrigenous deposits of the Yukhta Formation.

Three stages in the formation of deposits are distinguished: pre-Jurassic (development of weathering and karst along the Vendian-Cambrian carbonate layers); Jurassic (accumulation of Yukhta Deposits, intrusion of dikes, subvolcanic bodies, injection of brecciated rocks, development of potassium metasomatism and sulfidization in the rocks of the platform cover); and Late Neogene–Early Quaternary (weathering, intensive karst formation, development of oxidation zones with the redistribution of derivatives of the previous endogenous processes and the formation of gold-bearing deposits of the eluvial-karst type).



**Figure 9.** The structure of the Kuranakh ore deposit. After [7] with simplifications.

The detailed study of the ore-bearing pyrite-adularia-quartz and pyrite-quartz metasomatites recovered from clay-sand-limonite zones of oxidation and disintegration of the Kuranakh Deposits has led to the identification of two productive associations: (1) early fine-grained quartz with finely

dispersed gold in pyrite and (2) late medium-grained quartz with polysulfides (pyrite, chalcopyrite, galena, sphalerite, arsenopyrite, stibnite and visible (830–875 ‰) gold) [5]. The late association also contains Au-telluride mineralization, represented by altaite (PbTe), coloradoite (HgTe), calaverite (AuTe<sub>2</sub>), krennerite (AuAgTe<sub>2</sub>), sylvanite (AuAgTe<sub>4</sub>) and petzite (AuAg<sub>2</sub>Te<sub>3</sub>). Sylvanite and coloradoite occur in intergrowths, are more common than other tellurides [5], and constitute an elevated fraction in heavy concentrates together with pyrite, gold (790–900 ‰), arsenopyrite, stibnite, cinnabar and native silver. High concentrations of Te, Se and Hg were also observed in technological ore samples [7].

Fragments of calcite veins preserved in the oxidized ores have very high contents of native Au and so-called “mustard gold” within the abovementioned tellurides and selenides such as naumannite (Ag<sub>2</sub>Se), claustalite (PbSe) and timmanite (HgSe) as well as Zn, Pb, Ca, V, P and As tellurides. The inclusions in sulfides are dominated by cinnabar with very rare orpiment [5].

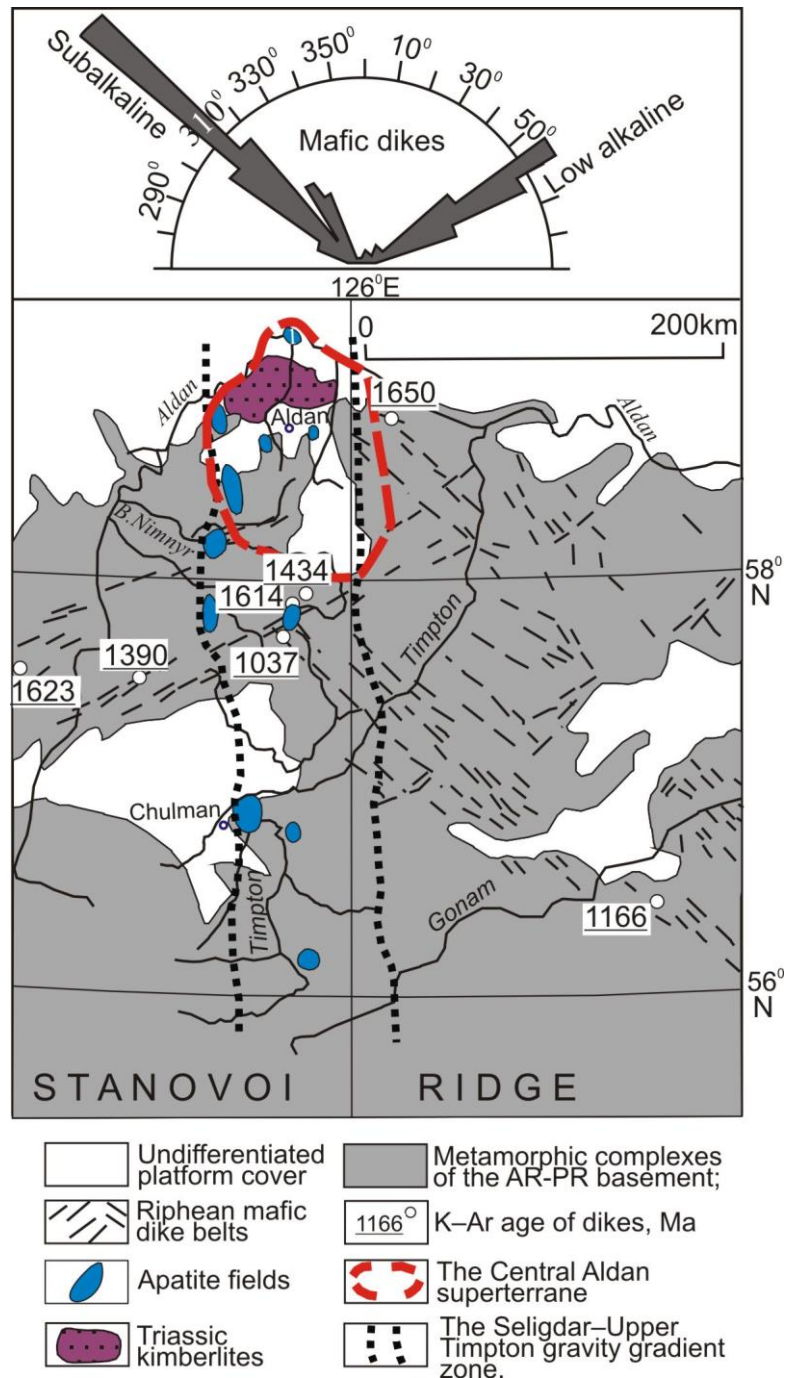
Finally, carbonate veinlets containing fine-grained pyrite and carbonaceous matter (10 and several hundred g/t of Au and Ag, respectively) were found under gold-bearing karst cavities at depths of 260–500 m [32]. The same level of noble metal content was found in bitumen [7].

### 3.2. Geophysical characteristics of the South Yakutia

The province’s area coincides with the sublatitudinal Baikal-Elkon-Ulkan global gravity gradient zones, separating the Aldan Shield from the East Siberian (Lena) megablock [41]. According to deep seismic tomography data, the megablock is characterized by a high-velocity lithosphere with a more than 100 km-thick ancient inactivated craton [59]. Large linear positive striped magnetic anomalies of meridional and NW orientations are determined. They seem to be controlled by deep faults and correspond to hidden linear bodies of mafic and ultramafic composition [60]. The thickness of the lithosphere of the Aldan Shield is estimated by geophysicists at 140–170 km, and that of the Earth’s crust is estimated at 35–40 km. The density maximum in the lithosphere and the Earth’s crust corresponds to a relative decrease in the density of the lithospheric mantle [21]. Several gravity steps of the second order of sublatitudinal (South Aldan) and submeridional (Olekma, Seligdar-Verkhnetimpon) strikes are observed in the province [61]. The Seligdar-Verkhnetimpon longitudinally oriented step (Figure 10) between the Amga and Tyrkanda zones of the tectonic melange is characterized by a lower thickness (up to 36–38 km) of the Earth’s crust with lower density, numerous apatite-bearing alkaline-ultrabasic massifs, the presence of an area of Triassic kimberlites [62] and large linear (Seligdar and Yakokut) graben-valleys spatially paired with deep magma-controlling faults. The relative average statistical level of  $\Delta g_a$  differs significantly from the West and East Aldan megablocks (–10 mGal and +30 mGal, respectively) [63].

A higher concentration of geophysical anomalies of different scale in the form of linear crustal and crustal-mantle decompression zones has been established in the middle part of the CAR. They are interpreted as tectonic rift zones, paleo-magmatic chambers and exposed and not exposed intrusions [64]. At depths of 10–32 km, isometric and oval gravity minimums interpreted as first-order magma chambers were found (Figure 11). Some of them are framed by zones of an “elevated” gravity field, probably corresponding to the hidden basic and ultrabasic rocks with roots at the bottom of the lithosphere at 200–220 km depth. At shallow depths (4–10 km), there are approximately 10 areas of low density corresponding to hidden granitoid intrusions in the CAR. The neighboring Central Aldan and Yakokut minimums of  $\Delta g$  anomalies with amplitudes of several

tens of mGal are caused by the cascades of large three-tiered paleomagnetic chambers at depths of 14–22, 4–10 and 0–3 km (Figure 11).

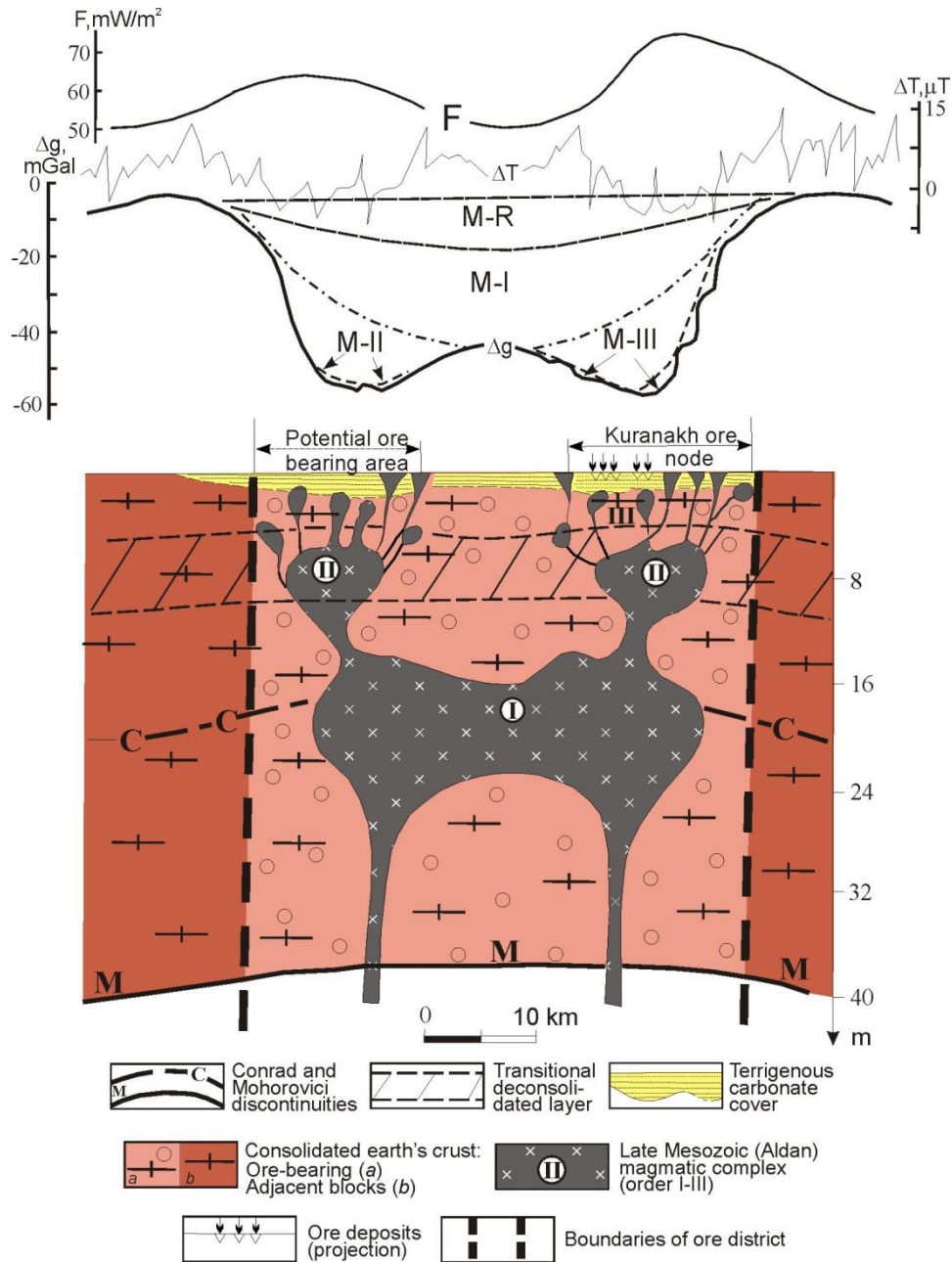


**Figure 10.** Riphean mafic dike belts, apatite fields (in carbonatites) and Triassic kimberlites in the Seligdar–Upper Timpston gravity gradient zone (Aldan Shield). After [61] with simplifications.

Seismic tomography provides additional data on deep sublithospheric levels of the region corresponding to the asthenosphere, transition zone and lower mantle [64,65]. They have revealed traces of a paleo-transform fault of northwestern orientation in the transition zone (410–660 km)



below the southeastern and northern parts of the Aldan Shield, defining a margin of the stagnated oceanic slab from the northeast [9]. The southeastern extension of this paleo-transform fault was evidenced by seismic tomography studies [66] both under the Sea of Okhotsk and at the bottom of the Pacific Ocean near the southeastern margin of the Kuril Island arc [15]. Such faults are known in the northwestern Pacific [18,67] and extend further to the southeast until the Shatsky uplift (Figure 1).



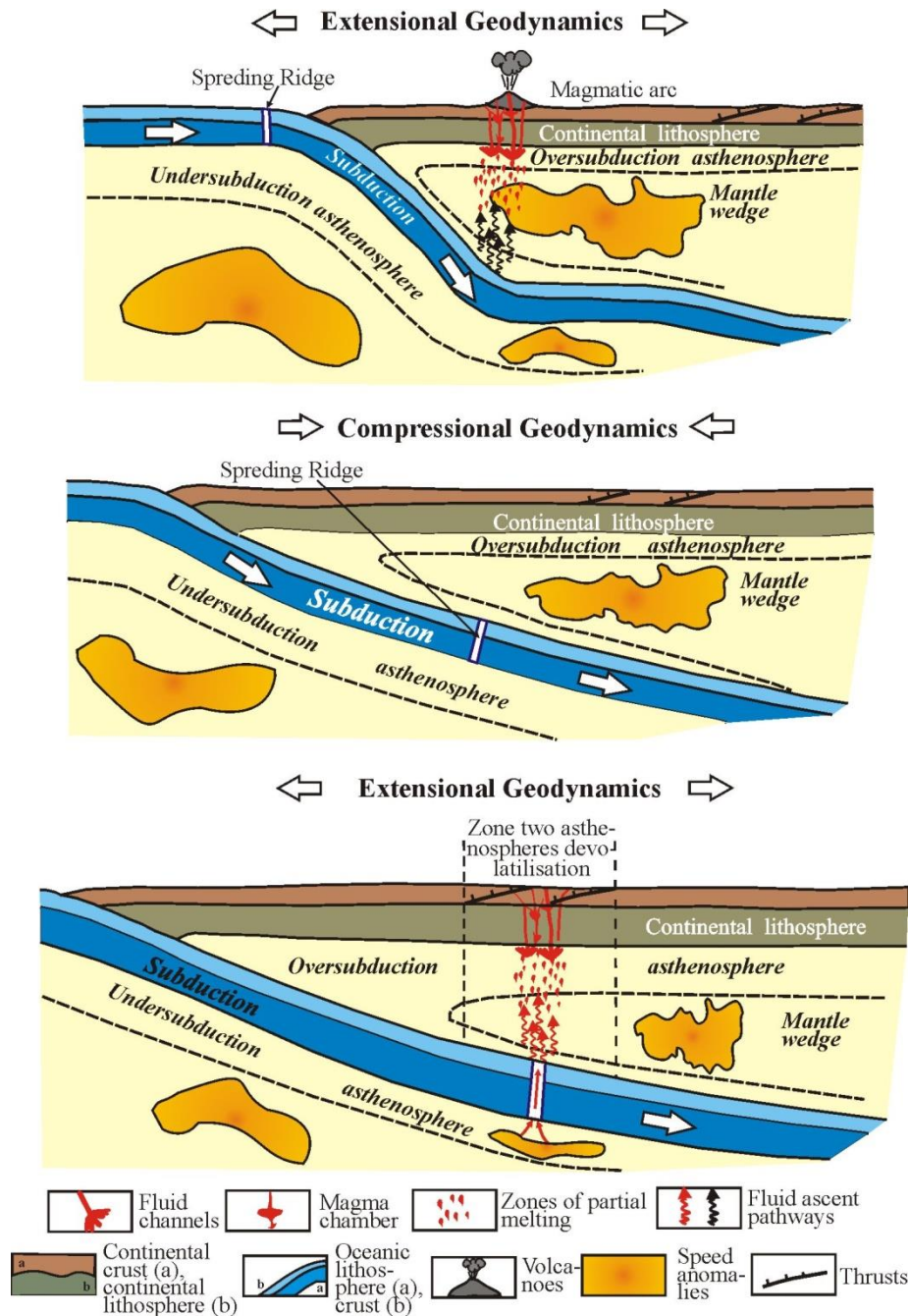
**Figure 11.** Generalized section of the Aldan gold-ore district as derived from geological and geophysical data, and curves of geophysical anomalies:  $\Delta g$ —observed and calculated gravity field (M-R—minimum for the Central Aldan roughly NS-trending regional fault; M-I, M-II, M-III—minimum for first-, second-, and third-rank crustal magma chambers);  $\Delta T$ —full vector magnetic field,  $F$ —high heat flow ( $\text{mW/m}^2$ ). Modified after [63].

#### 4. Discussion

The data on the geological and geophysical characteristics and ore contents of world-class noble metal provinces located on the convergent margins of the North Pacific presented in the previous sections unambiguously show that the provinces have a significant number of comparable indicators. The diversity of formational and mineral types of deposits in the area is obvious among the general metallogenic features. Au-PGE, Au-U, Au-skarn and skarnoid, Au-pyrite, Au-Cu-porphyry, Au-polymetal, Au-sulfide-quartz, Au-quartz, Au-Ag and Au-Sb-Hg deposits are present in addition to typomorphic Au-jasperoid deposits. The majority of them have undergone various degrees of supergene processing contributing to the formation of rich placers under appropriate geomorphological conditions. Not all types of deposits were found in each of the provinces. Additionally, not all provinces have large placers. However, it is obvious that one of the reasons for the wide diversity of deposits is the specific tectonic and geodynamic conditions of the ore-magmatic systems in the provinces.

The diversity of deposit types can be explained by the existence of a long-lived subcrustal Au source in the upper mantle [68]. The formation of Carlin-type world-class Au deposits involves two asthenospheric sources (Figure 12): the subslab source, which contributes to the metasomatic refertilization of the subslab lithospheric mantle, and the resulting subcrustal source, which leads to hot mantle upwelling. This upwelling is likely unrelated to lateral convection processes. The occurrence of decompression in areas influenced by large transform fault zones and buried spreading centers can result in the formation of melts in the suboceanic mantle and asthenosphere. These melts may contain reduced gases, including mantle He, and components of fluid-energetic phases. As these melts migrate through the mantle wedge, subcontinental asthenosphere, upper metasomatizing mantle and lower parts of Earth's crust, they can contribute to the formation of primary magmatic chambers. Ore-bearing volcanic-plutonic systems can then form above these chambers, creating favorable conditions for the localization of diffusive ore-magmatic systems. The Carlin-type Au deposits may occur in the remote porphyry part of these systems.

Despite a relatively equal (125 Ma) total lifetime of four-stage Mesozoic-Cenozoic magmatism within the compared marginal areas of the North Pacific, South Yakutia covers the period from the Triassic to the Late Cretaceous (100–225 Ma), and Nevada covers the period from the Late Jurassic (158 Ma) to the Oligocene (339 Ma) [27]. Magmatic formations are usually regarded as an indicative sign of ore-bearing areas. Accordingly, the ring-zoned platinum-bearing alkaline-ultramafic massifs (with a dunite core) in the South Yakutia province are responsible for the platinum-metal mineralization of the majority of gold-bearing ore-placer deposits [62]. Note also the relatively low appearance of Sb and Hg mineralization in the South Yakutia province, widely presented in the “Golden Triangle” of the PRC.



**Figure 12.** Model of the formation of the Carlin-type Au deposits.

Geologically and tectonically, the North Pacific is characterized by the location of the provinces in relatively mobile marginal parts of the platforms (North American, Siberian, South China), surrounded by folding belts. In layered ore-hosting sections of the cover of the provinces, the mineralization is largely concentrated in the areas where carbonate deposits are replaced by terrigenous-siliceous-volcanic deposits and where multistage oppositely oriented contrasting deformations and, consequently, numerous interlayer discontinuities and thrust faults in zones of deep long-lived faults into the upper mantle and transition zone are documented. Some researchers associate the origin of such faults with the Neoproterozoic orogeny [3,19], while others associate them with the existence of ancient aulacogens in the Archean craton basement [41]. In both cases, the deep faults were repeatedly reactivated under the influence of subsequent orogenic and subduction

processes and tectonic-magmatic activations. The long life of the faults is confirmed by the occurrence of volcano-plutonic formations of different ages (Triassic-Jurassic-Cretaceous-Eocene) near and above their junctions. The depth of their penetration is confirmed by the presence of kimberlite explosive pipes [62], ring-zoned (with a dunite core) platinum-bearing alkaline ultramafic massifs and the results of complex geophysical studies. They record the existence of orthogonal combinations of the gradient zones of the gravity field of the I and II orders in both South Yakutia and Nevada provinces. In South Yakutia Province, this combination is confirmed by the sublatitudinal orientation of the Baikal-Elkon-Ulkan (I order) and submeridional-Seligdar-Verkhnetimpon (II order) gradient zones. In Nevada, it is documented by the superposition of a large positive gravity anomaly known as the “Northern Nevada Rift” with higher-order gradient zones. Linear magnetic field anomalies are also found in the area [27]. In this regard, the presence of a large pluton (with a thickness of at least 10 km, 12–23 km wide and up to 50 km long) under the Goldstrike laccolith at depths from 3 (south) to 8–10 km (north) is important, according to [27], as the main heat source driving the hydrothermal systems of the Carlin and BME trends. A similar pluton whose derivatives control the placement of Au-jasperoid deposits in the Kuranakh cluster [63] has also been found in the South Yakutia province.

The comparative analysis of the seismic tomography data provides evidence of the existence of transform-type fault zones in both provinces. There is the Mendocino sublatitudinal transform fault zone under the northern border of the Nevada Province at the depth of stagnant slabs. It controls the distribution of the Getchell and Jerritt Canyon trend fields (Figure 3). The extension of the Juan de Fuca paleo-spreading center with a northwestern orientation initiated the formation of the mentioned magma chamber and is assumed to exist to the south from this transform fault zone. This magma chamber provided fluids and heat for the formation of the Carlin and Cortez (BME) trend deposits and probably the deposits of the Paquot area.

In South Yakutia Province, the influence of the transform fault zone on the formation of noble metal mineralization in the CAR and other parts of the Inagli-Konder-Feklistov magma-metallogenic belt was established [9]. A paleo-transform fault of northwestern orientation is traced in the mantle transition zone under the southeastern and northern parts of the Aldan Shield, the Sea of Okhotsk and the Pacific Ocean until the Kuril Island arc further to the southeast [15,18] (Figure 1).

A brief discussion of geological and geophysical data on the distribution of Carlin-type gold deposits resulted in a conclusion about the fundamental role of geodynamic factors in the origin and development of ore-magmatic systems that created Au-jasperoid mineralization in large metallogenic provinces of the North Pacific. Significant differences in the scale of the revealed gold mineralization of both provinces are explained by the existence of the Inagli-Konder-Feklistov magma-metallogenic belt in the South Yakutia province under the Asian continent and not only the Mendocino transform fault zone but also the Juan de Fuca paleo-spreading center under the North American continent.

## 5. Conclusions

The analysis of the geological settings of world-class noble metal provinces in the North Pacific and the main geodynamic factors of the formation of such provinces, based on tectonic, geophysical and seismic tomography studies, has confirmed the existence of transform fault zones in both provinces. They are recorded by seismic tomography in the transition zone (at depths of 410–670 km) in the form

of slab boundaries separating fragments of oceanic plates subducted into the mantle [39,65]. Toroidal convecting flows deliver fluids and heat from the underlying asthenosphere and undepleted mantle to the shallower mantle and lithosphere in these areas. Migrating upward through the mantle wedge to the overlying asthenosphere, such fluid-heat flows contributed to mantle metasomatism and the formation of primary magma chambers in the lower lithosphere. The subsequent migration of flows has led to the formation of ore-magmatic systems and localization of gold mineralization in favorable lithological-stratigraphic and structural conditions.

The existence of transform-type fault zones in the mantle transition zone was confirmed by seismic tomography at the western (California) coast of North America (Mendocino, Murray, etc.), at the eastern (Okhotsk) coast of Asia (Inagli-Konder-Feklistov zone) and the northern coast of Vietnam (fault zones of Ailaoshan and Red River). In each of them, toroidal flows at the slab margins provided the conditions for the formation of the corresponding deposits in the Earth's crust. This is confirmed by the Getchell and Jerritt Canyon (Nevada, USA) and Kuranakh (South Yakutia, Russia) trends (linear zones with the same type of deposits), as well as the Dian-Qian-Gui "Golden Triangle" of Southwest China.

### Use of AI tools declaration

The authors declare they have not used Artificial Intelligence (AI) tools in the creation of this article.

### Acknowledgments

Jeanette Shcheka and Svetlana Vasyukevich are thanked for their help with the work.

### Conflict of interest

All authors declare no conflicts of interest in this paper.

### References

1. Muntean JL (2018) Diversity in Carlin-Style Gold Deposits, *Reviews in Economic Geology*, SEG Inc, 1–363. <https://doi.org/10.5382/rev.20>
2. Muntean JL, Cline JS, Simon AC, et al. (2011) Magmatic–hydrothermal origin of Nevada's Carlin-type gold deposits. *Nature Geosci* 4: 122–127. <https://doi.org/10.1038/ngeo1064>
3. Cline JS, Hofstra AH, Muntean JL, et al. (2005) Carlin-Type Gold Deposits in Nevada: Critical Geologic Characteristics and Viable Models, *100th Anniversary Volume (1905–2005)*, SEG Inc Econ Geol, 451–484. <https://doi.org/10.5382/AV100.15>
4. Su WC, Dong WD, Zhang XC, et al. (2018) Carlin-Type Gold Deposits in the Dian-Qian-Gui "Golden Triangle" of Southwest China, In: Muntean JL, Author, *Diversity in Carlin-Style Gold Deposits*, 157–185. <https://doi.org/10.5382/rev.20.05>
5. Kim AA (2000) Gold-tellurium-selenium mineralization in Kuranakh Deposit (Central Aldan) [in Russian]. *Miner Soc Bull* 129: 51–57.

6. Bakulin YI, Buryak AE, Perestoronin AE (2001) *Carlin type gold mineralization (location pattern, genesis, geological basis of forecasting and estimation* [in Russian]. DVIMS NRD RF, Khabarovsk.
7. Vetluzhskikh VG, Kazansky VI, Kochetkov AY, et al. (2002) Central Aldan gold deposits. *Geol Ore Deposits* 44: 405–434. Available from: <https://www.pleiades.online/cgi-perl/search.pl?type=abstract&name=geolore&number=6&year=2&page=405>.
8. Khomich VG, Boriskina NG (2011) Main Geologic-Genetic Types of Bedrock Gold Deposits of the Transbaikal Region and the Russian Far East. Russia. *Russ J of Pac Geol* 5: 64–84. <https://doi.org/10.1134/S1819714011010040>
9. Khomich VG, Boriskina NG, Santosh M (2014) A geodynamic perspective of world-class gold deposits in East Asia. *Gondwana Res* 26: 816–833. <https://doi.org/10.1016/j.gr.2014.05.007>
10. Molchanov AV, Terekhov AV, Shatov VV, et al. (2017) Gold ore districts and ore clusters of the Adanian metallogenic province. *Reg Geol Metallog* 71: 93–111.
11. Leontev VI, Bushuev YY, Chernigovcev KA (2018) Samolazovskoe gold deposit (Central Aldan ore district): geological structure and mineralization of deep horizons. *Reg Geol Metallog* 75: 90–103.
12. Petrov OV, Molchanov AV, Terekhov AV, et al. (2018) Morozkinskoe gold deposit (geological structure and short story of the exploration). *Reg Geol Metallog* 75: 112–116. Available from: [https://elibrary.ru/download/elibrary\\_36457688\\_12396066.pdf](https://elibrary.ru/download/elibrary_36457688_12396066.pdf).
13. Minina OV (2019) Paleokarst role in Lebedinsky ore cluster gold orebodies localization, Yakutia [in Russian]. *Rudy i Metally* 4: 58–74. <https://doi.org/10.24411/0869-5997-2019-10032>
14. Arehart GB, Ressel M, Carne R, et al. (2013) A Comparison of Carlin-type Deposits in Nevada and Yukon. In: Colpron M, Bissig T, Rusk BG, et al., *Tectonics, Metallogeny, and Discovery: The North American Cordillera and Similar Accretionary Settings*, 389–401. Available from: <https://www.segweb.org/store/SearchResults.aspx?Category=SP17-PDF>
15. Khomich VG, Boriskina NG, Kasatkin SA (2019) Geology, magmatism, metallogeny, and geodynamics of the South Kuril Islands. *Ore Geol Rev* 105: 151–162. <https://doi.org/10.1016/j.oregeorev.2018.12.015>
16. Grebennikov AV, Khanchuk AI (2021) Geodynamics and magmatism of the pacific-type transform margins. aspects and discriminant diagrams [in Russian]. *Tikhookeanskaya Geologiya* 40: 3–24. Available from: [http://itig.as.khb.ru/POG/2021/n\\_1/pdf/Grebennikov\\_RGB.pdf](http://itig.as.khb.ru/POG/2021/n_1/pdf/Grebennikov_RGB.pdf)
17. Khomich VG, Boriskina NG (2021) Eventual solution to the problems of gold ore trends localization in the Carlin province (Nevada, USA). *Int J Earth Sci (Geol Rundsch)* 110: 2043–2055. <https://doi.org/10.1007/s00531-021-02056-2>
18. Khomich VG, Boriskina NG (2021) Petroleum potential of the Uchur zone of the Aldan antecline (Siberian Platform). *J Petrol Sci Eng* 201: 108501. <https://doi.org/10.1016/j.petrol.2021.108501>
19. Hronsky JMA, Groves DI, Loucks RR, et al. (2012) A unified model for gold mineralisation in accretionary orogens and implications for regional-scale exploration targeting methods. *Miner Deposita* 47: 339–358. <https://doi.org/10.1007/s00126-012-0402-y>
20. Zhu J, Zhang ZC, Santosh M, et al. (2020) Carlin-style gold province linked to the extinct Emeishan plume. *EPSL* 530: 115940. <https://doi.org/10.1016/j.epsl.2019.115940>
21. Khanchuk AI (2006) *Geodynamics, magmatism, and metallogeny of the Russian East* [in Russian]. Dalnauka, Vladivostok.

22. Hofstra AH, Cline JS (2000) Characteristics and models for Carlin-type gold deposits, In: Hagemann SG, Brow PE, (Eds.), *Gold in 2000*, 163–220. Available from: <https://www.segweb.org/Store/detail.aspx?id=EDOCREV13CH05>.
23. Cline JS (2018) Nevada's Carlin-Type Gold Deposits: What We've Learned During the Past 10 to 15 Years. In: Muntean JL, *Diversity in Carlin-Style Gold Deposits*, 20: 7–38. <https://doi.org/10.5382/rev.20.01>
24. Manning AH, Hofstra AH (2017) Noble gas data from Goldfield and Tonopah epithermal Au-Ag deposits, ancestral Cascades Arc, USA: Evidence for a primitive mantle volatile source. *Ore Geol Rev* 89: 683–700. <http://dx.doi.org/10.1016/j.oregeorev.2017.06.023>
25. Weil AB, Yonkee WA (2012) Layer-parallel shortening across the Sevier fold-thrust belt and Laramide foreland of Wyoming: spatial and temporal evolution of a complex geodynamic system. *EPSL* 357–358: 405–420. <http://dx.doi.org/10.1016/j.epsl.2012.09.021>
26. Wang J, Li CF (2015) Crustal magmatism and lithospheric geothermal state of western North America and their implications for a magnetic mantle. *Tectonophysics* 638: 112–125. <http://dx.doi.org/10.1016/j.tecto.2014.11.002>
27. Ressel MW, Henry CD (2006) Igneous geology of the Carlin trend, Nevada: development of the Eocene plutonic complex and significance for Carlin-type gold deposits. *Econ Geol* 101: 347–383. <https://doi.org/10.2113/gsecongeo.101.2.347>
28. Kuchai VK, Vesson RL (1980) Fixed hot zone, types of orogenesis and Cenozoic tectonics of the USA West. *Geotectonics* 2: 49–62
29. Berger VI, Mosier DL, Bliss JD, et al. (2014) Sediment-hosted gold deposits of the world—Database and grade and tonnage models, Open-File Report 2014–1074. Available from: <http://dx.doi.org/10.3133/ofr20141074>.
30. Bray du EA, John DA, Colgan JP, et al. (2019) Morgan, Petrology of Volcanic Rocks Associated with Silver-Gold (Ag-Au) Epithermal Deposits in the Tonopah, Divide, and Goldfield Mining Districts, Nevada. Available from: <https://pubs.usgs.gov/sir/2019/5024/sir20195024.pdf>.
31. Fithian MT, Holley EA, Kelly NM (2018) Geology of Gold Deposits at the Marigold Mine, Battle Mountain District, Nevada, In: Muntean JL, *Diversity in Carlin-Style Gold Deposits*, 121–156. <https://doi.org/10.5382/rev.20.04>
32. Boitsov VE, Pilipenko GN (1998) Gold and uranium in the Mesozoic hydrothermal deposits of the Central Aldan region (Russia) [in Russian]. *Geol Ore Deposits* 40: 354–369.
33. Shatova NV, Molchanov AV, Terekhov AV, et al. (2019) Ryabinovoe copper-gold-porphyry deposit (Southern Yakutia): geology, noble gases isotope systematics and isotopic (U-PB, RB-SR, RE-OS) dating of wallrock alteration and ore-forming processes. *Regionalnaya Geologiya i Metallogeniya* 77: 75–97. Available from: [https://elibrary.ru/download/elibrary\\_37422881\\_84522683.pdf](https://elibrary.ru/download/elibrary_37422881_84522683.pdf).
34. Van der Meer DG, van Hinsbergen DJJ, Spakmana W (2018) Atlas of the underworld: Slab remnants in the mantle, their sinking history, and a new outlook on lower mantle viscosity. *Tectonophysics* 723: 309–448. <https://doi.org/10.1016/j.tecto.2017.10.004>
35. Gainanov AG, Krasny LI, Stroyev PA (1979) *Explanatory note to gravimetric maps of the Pacific Ocean and the Pacific Ocean mobile belt* [in Russian]. VSEGEI, Leningrad.
36. Chen CX, Zhao DP, Wu SG (2015) Tomographic imaging of the Cascadia subduction zone: Constraints on the Juan de Fuca slab. *Tectonophysics* 647–648: 73–88. <http://dx.doi.org/10.1016/j.tecto.2015.02.012>

37. Sigloch K, McQuarrie N, Nolet G (2008) Two-stage subduction history under North America inferred from finite-frequency tomography. *Nature Geosci* 1: 458–462. <https://doi.org/10.1038/ngeo231>
38. Faccenna C, Becker W, Lallemand S, et al. (2010) Subduction-triggered magmatic pulses: A new class of plumes? *EPSL* 299: 54–68. <https://doi.org/10.1016/j.epsl.2010.08.012>
39. James DE, Fouch MJ, Carlson RW, et al. (2011) Slab fragmentation, edge flow and the origin of the Yellowstone hotspot track. *EPSL* 311: 124–135. <https://doi.org/10.1016/j.epsl.2011.09.007>
40. Sigloch K (2011) Mantle provinces under North America from multifrequency P wave tomography. *Geochem Geophys Geosyst* 12: Q02W08. <https://doi.org/10.1029/2010GC003421>
41. Parfenov LM, Kuzmin MI (2001) *Tectonics, geodynamics, and metallogeny of the area of republic of Sakha (Yakutiya)* [in Russian]. Nauka, Moscow.
42. Khomich VG, Boriskina NG (2013) Large gold-ore districts of Southeast Russia: features of position and structure. *Lithosphere* (Russian). 1: 128–135. Available from: [https://elibrary.ru/download/elibrary\\_19096337\\_71208627.pdf](https://elibrary.ru/download/elibrary_19096337_71208627.pdf).
43. Kazansky VI (2004) The unique Central Aldan gold-uranium ore district (Russia). *Geol Ore Deposits* 46: 167–181.
44. Dick IP (1998) Gold placers-giants of Aldan [in Russian]. *Otechestvennaya Geologiya* 3: 47–49.
45. Maximov EP, Nikitin VM, Uytov VI (2010) The Central Aldan gold-uranium ore magmatogenic system, Aldan-Stanovoy Shield, Russia. *Russ J Pac Geol* 4: 95–115. <https://doi.org/10.1134/S1819714010020016>
46. El'yanov AA, Andreev GV (1991) *Magmatism and metallogeny of multistagely activated cratonic areas* [in Russian]. Nauka, Novosibirsk.
47. Polin VF, Mitsuk VV, Khanchuk AI, et al. (2012) Geochronological limits of subalkaline magmatism in the Ket-Kap-Yuna igneous province, Aldan Shield. *Dokl Earth Sci* 442: 17–23. <https://doi.org/10.1134/S1028334X12010096>
48. Shatov VV, Molchanov AV, Shatova NV, et al. (2012) Petrography, geochemistry and isotopic (U-Pb and Rb-Sr) dating of alkaline magmatic rocks of the Ryabinovy massif (South Yakutia) [In Russian]. *Regionalnaya Geologiya i Metallogeniya* 51: 62–78.
49. Samovich DA, Tsaruk II, Kokarev AA, et al. (2012) Uranium mineral-raw material base of East Siberia, Irkutsk: Glazkovskaya tipografiya.
50. Kononova VA, Pervov VA, Bogatikov OA, et al. (1995) Mesozoic potassic magmatism of Central Aldan: geodynamics and genesis [in Russian]. *Geotektonika* 3: 35–45
51. Kazansky VI, Maximov EP, (2000) Geological setting and development history of the El'kon uranium ore district (Aldan Shield, Russia). *Geol Ore Deposits* 42: 189–204.
52. Ponomarchuk AV, Prokop'ev IR, Svetlitskaya TV, et al. (2019)  $^{40}\text{Ar}/^{39}\text{Ar}$  geochronology of alkaline rocks of the Inagli massif (Aldan Shield, Southern Yakutia). *Russ Geol Geophys* 60: 33–44. <https://doi.org/10.15372/RGG2019003>
53. Yanovsky VM, Chmyrev AV, Sorokin AB (1995) Geodynamic Models of Gold in the Regions of Tectono-Magmatic Activization [in Russian]. *Rudy i Metally* 6: 45–51.
54. Ibragimova EK, Radkov AV, Molchanov AV, et al. (2015) The results of U-Pb (SHRIMP II) isotope dating of zircons from dunite from massif Inagli (Aldan Shield) and the problem of the genesis of concentrically-oned complexes. *Regionalnaya Geologiya i Mmetallogeniya* 62: 64–78. Available from: [https://elibrary.ru/download/elibrary\\_24251614\\_51302773.pdf](https://elibrary.ru/download/elibrary_24251614_51302773.pdf).



55. Okrugin AV, Yakubovich OV, Ernst R, et al. (2018) *Geology and Mineral Resources of the North-East of Russia* [in Russian]. NEFU, Yakutsk.
56. Khomich VG, Boriskina NG (2016) Essence of the late mesozoic ore-magmatic systems of Aldan Shield. *Lithosphere* (Russian) 2: 70–90. Available from: [https://elibrary.ru/download/elibrary\\_26008762\\_33747994.pdf](https://elibrary.ru/download/elibrary_26008762_33747994.pdf).
57. Ronkin YL, Efimov AA, Lepikhina GA, et al. (2013) U-Pb dating of the baddeleyite-zircon system from Pt-bearing dunite of the Konder massif, Aldan Shield: New data. *Dokl Earth Sci* 450: 607–612. <https://doi.org/10.1134/S1028334X13060135>
58. Kopulov MI (2010) Future views for the gold exploration in the Allakh-Yun metallogenic area, Russian Far East [in Russian]. *Otechestvennaya Geologiya* 3: 23–32. Available from: <https://elibrary.ru/item.asp?id=14672498>.
59. Shatkov GA, Volsky AS (2004) Tectonics, Deep Structure, and Minerageny of the Amur River Region and Neighboring Areas. *Izdatelstvo VSEGEI, St. Petersburg*, 1–190.
60. Glebovitsky VA, Khil'tova VY, Kozakov IK (2008) tectonics of the Siberian Craton: interpretation of geological, geophysical, geochronological, and isotopic geochemical data. *Geotectonics* 42: 8–20. <https://doi.org/10.1134/S0016852108010020>
61. Khomich VG, Boriskina NG (2010) Structural position of large gold ore districts in the Central Aldan (Yakutia) and Argun (Transbaikalia) superterrane. *Russ Geol Geophys* 51: 661–671. <https://doi.org/10.1016/j.rgg.2010.05.007>
62. Razin LV, Vasyukov VS, Izbekov ED, et al. (1994) *Russian Platinum. Developmental problems of mineral and raw materials of platinum metals* [in Russian]. Geoinformark, Moscow.
63. Abramov VA (1995) *Deep structure of the Central Aldan region* [in Russian]. Dalnauka, Vladivostok.
64. Maruyama S, Santosh M, Zhao D (2007) Superplume, supercontinent, and post-perovskite: Mantle dynamics and antiplate tectonics on the Core-Mantle Boundary. *Gondwana Res* 1: 7–37. <http://dx.doi.org/10.1016/j.gr.2006.06.003>
65. Zhao D, Pirajno F, Dobretsov NL, et al. (2010) Mantle structure and dynamics under East Russia and adjacent regions. *Russ Geol Geophys* 51: 925–938. <https://doi.org/10.1016/j.rgg.2010.08.003>
66. Koulakov IY, Dobretsov NL, Bushenkova NA, et al (2011) Slab shape in subduction zones beneath the Kurile–Kamchatka and Aleutian arcs based on regional tomography results. *Russ Geol Geophys* 52: 650–667. <https://doi.org/10.1016/j.rgg.2011.05.008>
67. Norton IO (2007) Speculations on Cretaceous tectonic history of the northwest Pacific and a tectonic origin for the Hawaii hotspot. *GSA Special Papers*, The Geological Society of America, 451–470. [https://doi.org/10.1130/2007.2430\(22\)](https://doi.org/10.1130/2007.2430(22))
68. Richards JP (2009) Postsubduction porphyry Cu-Au and epithermal Au deposits: Products of remelting of subduction-modified lithosphere. *Geology* 37: 247–250. <https://doi.org/10.1130/G25451A.1>



AIMS Press

© 2023 the Author(s), licensee AIMS Press. This is an open access article distributed under the terms of the Creative Commons Attribution License (<http://creativecommons.org/licenses/by/4.0>)